Entrainment as a means of controlling phase waves in populations of coupled oscillators

Jonas S. Juul,[1] Sandeep Krishna,[2,*] and Mogens H. Jensen[1,†]
[1]*Niels Bohr Institute, University of Copenhagen, Blegdamsvej 17, Copenhagen 2100-DK, Denmark*
[2]*Simons Centre for the Study of Living Machines, National Centre for Biological Sciences, GKVK Campus, Bellary Road, Bangalore 560065, India*

(Received 22 May 2018; published 21 December 2018)

We explore waves and entrainment in a model of coupled oscillators, inspired from the cellular oscillators in the presomitic mesoderm (PSM) of mice. The internal clock in each cell is based on a negative feedback loop which couples to the clocks of neighboring cells through a Notch mechanism. We investigate how a morphogen gradient in the mesoderm, which affects the period of oscillating cells, gives rise to phase waves traveling from the posterior to the anterior part of the PSM. We show that the phase waves can be entrained by an external periodic variation in this morphogen and also observe that multiple oscillatory solutions can coexist in the cell population. Together, these provide a way to potentially control phase waves and thereby manipulate somite patterning in embryos, based on entrainment properties of coupled nonlinear oscillators.

DOI: 10.1103/PhysRevE.98.062412

I. INTRODUCTION

Biological oscillators are ubiquitous in a wide range of systems from the molecular level up to macroscopic scales and play a fundamental role in how living systems function. These include ultradian biological clocks (period less than 24 h) that affect tumor growth [1–5] or vertebrae precursors in the vertebrate embryo [6–15] and the circadian clocks (period of approximately 24 h) that coordinate rhythms in mammalian physiology to the day-night cycle [16–18].

A natural task is to investigate ways to control the oscillations. Dynamical systems theory tells us that an oscillator can be entrained if it is driven by an external, periodic signal [19–23]. If the external periodic signal is characterized by a period T_{force} and a "strength" K_{force}, then certain combinations of the parameters $(T_{\text{force}}, K_{\text{force}})$ will successfully entrain the oscillator to have the period T_{force} or a rational multiple of this: $T_{\text{force}}P/Q$ with P and Q being positive integers. The region of this parameter space in which the oscillator is entrained and oscillates with period $T_{\text{force}}P/Q$ is referred to in the dynamical systems literature as a $P{:}Q$ Arnold tongue [24].

Entrainment of biological oscillators has been studied in several biological cases [25–34], with well-known, crucial functions such as the coordination of various rhythms to the day-night cycle. One biological process where oscillators are of fundamental importance is *somitogenesis*, the formation of vertebrae precursors in vertebrate embryos. In the vertebrate embryo, somites, the precursors of vertebrae, are periodically formed in the presomitic mesoderm (PSM) [35]. The PSM consists of a population of interacting stem cells [36], which we will refer to as PSM cells. Geometrically, the PSM can be described by an anteroposterior axis, where somites form in the anterior PSM and new PSM cells are continuously added in the posterior PSM [37]. Each PSM cell is an ultradian oscillator [38], exhibiting rhythmic pulsations in several pathways until it arrives at the anterior end of the PSM where it eventually becomes part of a newly formed somite.

Somitogenesis has been studied in great detail in particular in zebrafish, chicks, and mice. The exact mechanism behind somite formation is not known. Cooke and Zeeman [8] developed a famous framework, the "Clock and Wavefront Model," in which oscillating cells ("clocks") encounter a wavefront which moves from the anterior to the posterior PSM, thereby causing the cells to form somites. This mechanism depends on global morphogen gradients and has recently been challenged in theoretical and experimental studies which suggest, instead, mechanisms based on local reaction-diffusion behavior [39] or on interactions between several intracellular clocks [40]. Although the somite formation mechanism remains elusive, waves of protein expression have been observed to travel through the population of somite precursor cells from the posterior to the anterior PSM, and in all three species, the arrest of these waves in the anteriormost PSM has been found to coincide with the formation of a new somite [41–43]. Hence, we hypothesize that controlling the wave pattern, which is intimately linked to the individual cellular oscillators, may lead to controlling the spatial pattern of somites.

Recently, experiments have concluded that presomitic mesoderm cells in mice can be entrained [44] by external periodic variations in pathway modulators, and for this reason, theoretical studies of observable phenomena related to the entrainment of coupled, oscillating cells are important. Especially, studies focusing on the control of phase waves should be encouraged. In this paper, we take a previously proposed minimal model for the internal clock in PSM cells and add a coupling to achieve a limit cycle oscillator that is coupled to the oscillators in neighboring cells. We show that imposing a linear morphogen gradient gives rise to period and amplitude gradients across the PSM that are similar to what is observed experimentally. We then simulate an experiment in

*sandeep@ncbs.res.in
†mhjensen@nbi.dk

which the morphogen concentration is varied periodically in each cell in the PSM and find that this can entrain the traveling phase waves, thereby providing control over the wave pattern. Finally, we study entrainment of cell populations consisting of cells with similar natural frequencies. This corresponds to populations of cells that originate from the same position in the PSM. We find that when the external entraining signal forces the cellular oscillators into a region of overlapping Arnold tongues, multiple oscillatory solutions coexist. This generalizes a recent observation of coexisting oscillatory solutions in the NF-κB system [45]. In our case unlike the NF-κB case, cells are coupled in space, and thus coupled cells may be entrained to different limit cycles, which might manifest in the spatial pattern of somites.

The remainder of this paper is structured as follows: In Sec. II we describe our model of coupled PSM cells and their oscillatory behavior. In Sec. III we present our results in three subsections: in Sec. III A we show that a gradient of Wnt3a in this model leads to period and amplitude gradients in the PSM, resulting in traveling phase waves; in Sec. III B we vary the Wnt3a level in each PSM cell periodically and thereby entrain the traveling phase waves; Sec. III C deals with entrained populations of similar cells leading to coexisting oscillatory solutions. In Sec. IV we discuss the validity and implications of our results.

II. MODEL OF COUPLED, OSCILLATING CELLS

We aim to obtain a limit cycle oscillator with a parameter corresponding to the level of a morphogen gradient across the PSM, which we can use to study the possible effects of entrainment of oscillating cell populations. The internal clock in each cell is modeled by a negative feedback loop involving Axin2, β-catenin, and Axin2 messenger RNA, as was suggested in Refs. [14,46,47]. Several experiments have concluded that PSM cells coordinate their oscillations with their neighbors, and that Notch is the key in the coupling mechanism between cells in the PSM [11,13,48,49]. For this reason, we couple cells through the concentration of Notch in neighboring cells. It is unknown what mediates the cross talk between the Wnt pathway (the internal clock in our model) and the Notch pathway. We choose glycogen synthase kinase-3beta (GSK3β) in this model because experiments have indicated that GSK3β can bind to, and phosphorylate, Notch in other biological systems [50,51] and is involved in a destruction complex [52,53] along with β-catenin and Axin1 (which is functionally equivalent to Axin2 [54]). Thus, a coupling of cells via Notch interaction with GSK3β is biologically plausible.

Our model of interacting cells [Fig. 1(a)] is formulated in terms of a set of delay differential equations. For each cell, we keep track of the concentration of β-catenin, Axin2 mRNA, Axin2, and Notch, abbreviated B, A_m, A, and N, respectively. GSK3β enters effectively into our description via a parameter G_{tot} that sets the total amount of GSK3β, summing its concentration in free form and as part of the destruction complex. We assume that the Notch level which affects a given cell is dependent on the combined level of the Notch concentrations of the neighboring cells, $\sum_j N_j$. Recently it was found that a time delay in the coupling between cells can ensure defect-free patterning [55]. We incorporate such a delay in the production terms of Notch. The model then takes the form

$$\frac{dB_i}{dt} = S - \frac{\lambda G_t}{K_{BAG}} \frac{B_i A_i}{1 + \frac{N_i}{K_{NG}} + \frac{A_i}{K_{AG}}}, \tag{1}$$

$$\frac{dA_{m,i}}{dt} = c_{tsA} B_i^2 - \frac{A_{m,i}}{\tau_{Am}}, \tag{2}$$

$$\frac{dA_i}{dt} = c_{tlA} A_{m,i} - \nu L_{tot} \frac{A_i}{\frac{c_{b[AL]}+\nu}{c_{f[AL]}} + A_i}, \tag{3}$$

$$\frac{dN_i}{dt} = p_0 + \frac{\alpha k^n}{k^n + I_i(t-\tau)^n} - \frac{\epsilon G_{tot}}{K_{NG}} \frac{N_i}{1 + \frac{A_i}{K_{AG}} + \frac{N_i}{K_{NG}}}, \tag{4}$$

where i is an index that labels the cells. In the Notch equation, $I_i(x)$ is a coupling function given by

$$I_i(x) = \begin{cases} N_{i-1}(x) + N_{i+1}(x) & \text{if } 1 < i < N, \\ 2N_{i+1}(x) & \text{if } i = 1, \\ 2N_{i-1}(x) & \text{if } i = N. \end{cases} \tag{5}$$

τ is the delay in cell-to-cell signaling, p_0 a basic production rate, and $p_0 + \alpha$ is the maximal production rate.

All values of the parameters are listed in Table I. ν is the parameter which is proportional to the Wnt3a level of the cell [47]. In Fig. 1(b) the period of two coupled cells is plotted as a function of ν. This is the only parameter which we allow to vary from cell to cell. In each simulation, we will state the ν distribution for the particular study of interest. In Fig. 1(c) we show the time to synchronization of two cells with identical parameters and random initial conditions, as a function of the delay τ. The cells synchronize only for an interval of large τ values. For the remaining τ values, the cells tend to oscillate completely out of phase with each other. We choose $\tau = 25$ min for all cells in all simulations since experiments have shown that Notch helps synchronize the oscillations of cells [11,13,48,49].

Geometrically, we will approximate the PSM to be a line of cells, each connected only to two neighbors on either side of it. It has been observed that there is a gradient of Wnt3a over the PSM [14,42]. This correlates with the gradient of the oscillation period in the PSM. In our model, the ν parameter is proportional to the Wnt3a level in the cell [47]. Hence, we will simulate a presomitic mesoderm using a gradient in ν, going from high ν in the posterior PSM to low ν in the anterior PSM [Fig. 1(d)].

Experimentally, the period has been found to increase linearly from posterior (with period around 130 min) to anterior [42], the period being approximately 25%–30% longer in the anterior than in the posterior. The period in our model (1)–(4) is shorter [Fig. 1(b)], but since this model is derived from a larger model [47], which did have the correct period length, this seems to be a result of losing delay when simplifying from eight to three differential equations for the core clock. Hence, we do not consider this to be of importance. From our simulations, we find that a ν gradient decreasing linearly from

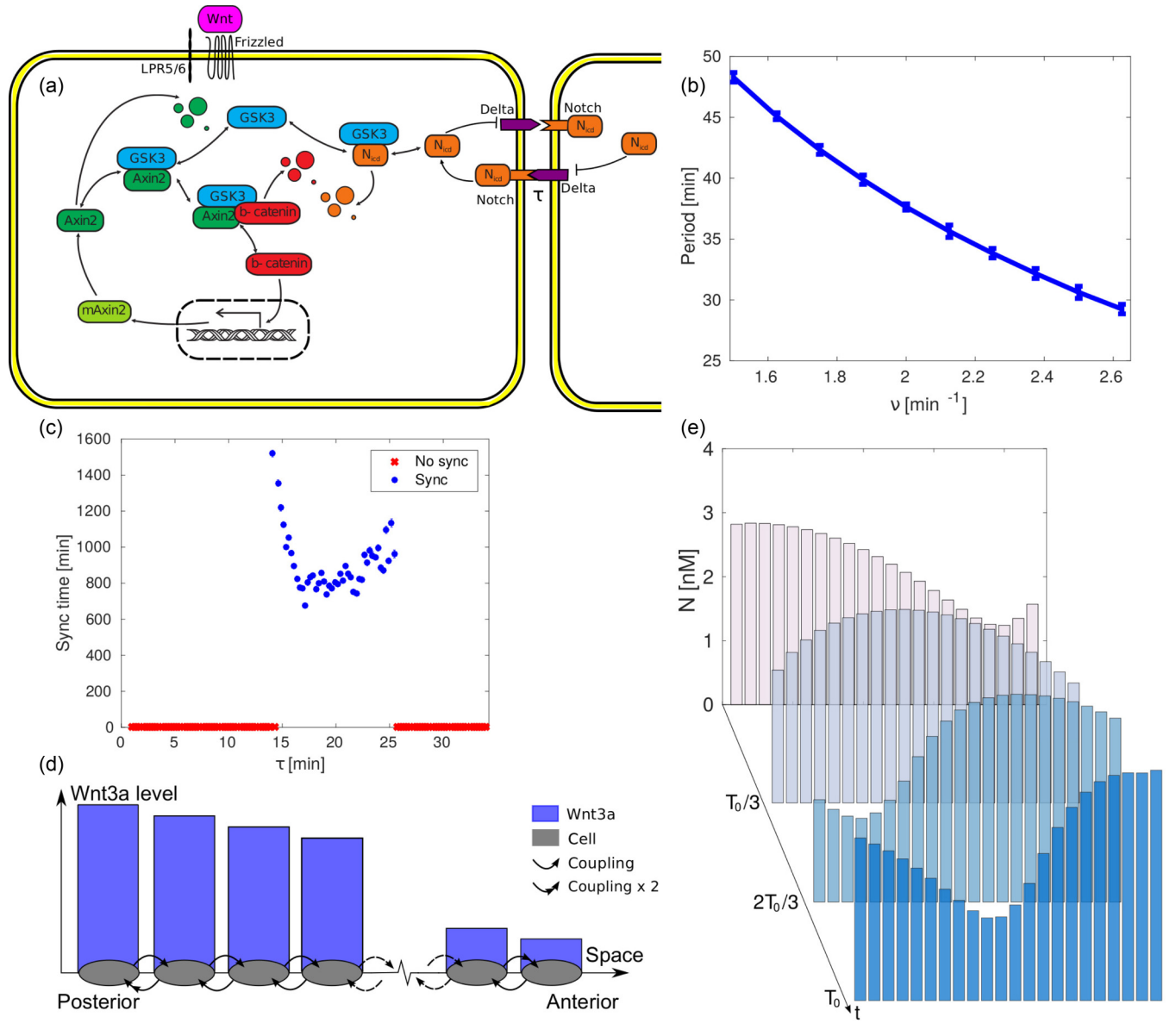

FIG. 1. *Basic characteristics of our model of interacting PSM cells.* (a) Schematic of the components and interactions in our model. The internal clock is based on the Axin2-β-catenin negative feedback loop, and neighboring cells are coupled with a delay τ through their Notch levels. Notch is phosphorylated by GSK3β internally in the cell. (b) The period of two coupled cells as a function of the parameter ν in Eqs. (1)–(5) [with $N = 2$, making $I_1(t-\tau) = 2N_2(t-\tau)$ and $I_2(t-\tau) = 2N_1(t-\tau)$], which is proportional to the Wnt3a level in the cells. (c) The time before synchronization of two coupled cells with identical parameters and initial conditions drawn uniformly at random from the interval [0, 10] nM for all variables. Each data point is averaged over 20 simulations. If cells failed to synchronize in any one of these simulations, the data point was defined as 0 ("No sync"). The plot shows that the delay needs to be in a specific range for the cells to synchronize. (d) Implementation of the model when simulating a PSM. Cells are placed on a line and couple to their nearest neighbors. Outermost cells have only a single spatial neighbor. As a boundary condition, we let the outermost cells couple to two copies of this neighbor. A linear Wnt3a gradient is placed over the line: posterior cells have a higher Wnt3a level than anterior cells. (e) Phase wave resulting from simulation of the model implemented as shown in (d), with the anterior period being $\approx$30% longer than the posterior period. Waves travel from posterior to anterior, with the amplitude of the Notch expression growing towards the anterior. This is in agreement with experimental observations [42].

posterior to anterior,

$$\nu_i = \nu_{\text{posterior}} + (\nu_{\text{anterior}} - \nu_{\text{posterior}})\frac{i-1}{N-1}, \qquad (6)$$

with $\nu_{\text{posterior}} = 2.500$ min^{-1} to $\nu_{\text{anterior}} = 2.125$ min^{-1} creates a gradient in the period with the correct fractional difference between posterior and anterior. A simulation with this type of ν gradient, and all initial protein concentrations equal to 2 nM, yields phase waves going from posterior to anterior [Fig. 1(e)]. In the following section, we will examine these waves in more detail.

TABLE I. *Parameters for the model of coupled PSM cells.* The first two parameters, K_{AG} and S, were chosen to be realistic values, from Jensen *et al.* [47,56]. The next three, c_{tsA}, c_{tlA}, and τ_{Am}, were chosen to be the estimated values of Jensen *et al.* [47]. K_{NG} was chosen to be one third of the size of K_{AG}, and λG_{tot} and ϵG_{tot} to have the same magnitude as K_{NG}. p_0 and α were chosen to be 0.5 nM min^{-1} each such that the maximal production rate of Notch is 1 nM min^{-1}. The three parameters $c_{f[AL]}$, $c_{b[AL]}$, and L_{tot} were chosen such that terms in Eqs. (1)–(4) had the same values as in the original model [47]. The next three parameters were chosen from parameter scans: ν (which is proportional to the Wnt3a level in the simulated cell) such that the period difference between posterior and anterior is ∼30% [Fig. 1(b)], and k and τ such that two coupled cells with the same parameters synchronize. When reducing the single-cell model from eight variables [47] to three variables [38], the final parameter, K_{BAG}, was given in terms of several parameters from the larger model. The value of the parameter was chosen such that the known realistic values of its constituents were used. The value of one of its constituents (called $c_{b,C}$) was determined such that two coupled cells with the same parameters synchronized their oscillations.

Parameter	Process	Default value
K_{AG}	Dissociation constant of G and A into the complex $[GA]$	6 nM
S	Constant source of β-catenin	0.4 nM min^{-1}
c_{tsA}	Transcription of Axin2 gene	0.7 nM^{-1} min^{-1}
c_{tlA}	Translation of Axin2 mRNA	0.7 min^{-1}
τ_{Am}	Average lifetime of Axin2 mRNA	40 min
K_{NG}	Dissociation constant of $[NG]$ and N, G	2 nM
$G_{tot}\epsilon$	Total G level times constant	2 nM min^{-1}
$G_{tot}\lambda$	Total G level times constant	2 nM min^{-1}
α	Constant in numerator of coupling term	0.5 nM min^{-1}
p_0	Constant production rate of Notch	0.5 nM min^{-1}
n	Hill coefficient	1
$c_{f[AL]}$	Binding of A to L	250 nM^{-1} min^{-1}
$c_{b[AL]}$	Dissociation of $[AL]$ into A and L	2 min^{-1}
L_{tot}	Total L level	2.8 nM
ν	Degradation of Axin2 in $[AL]$ complex (Wnt level included)	2.125–2.500 min^{-1}
τ	Delay in cell-cell coupling	1 nM min^{-1}
k	Constant in denominator of coupling term	2 nM
K_{BAG}	Dissociation constant of $[BAG]$ and B, A, G	2.48 nM^2

III. RESULTS

A. Traveling phase waves along the PSM in the absence of external forcing

We first explore the phase waves that can travel along the PSM in our model. The spatial implementation of the coupling between cells [Eqs. (1)–(4)] is shown in Fig. 1(d) (posterior being the leftmost part of the line). All cells are assigned the same parameter values except that the ν parameter is varied as described above. All cells are given the same initial conditions by setting all initial concentrations to 2 nM. In Fig. 1(e) we show that phase waves appear in the system after an initial transient period. Similar traveling waves have also been observed previously in Ref. [57], which differs from our model in two ways: it implements the PSM as a continuous line rather than a discrete set of cells as in our model and focuses on phase oscillators rather than limit-cycle oscillators.

In our model, after a transient period, cell trajectories lie on limit cycles. These are shown in Figs. 2(a) and 2(b). We see that the amplitude of oscillations in the variables N and A becomes larger the more anterior a cell is located. Experimentally, Notch oscillations have been reported to increase in amplitude in a similar way [42].

In Fig. 2(c) the oscillations in Notch concentrations of all cells are plotted as a function of time. A phase wave travels from posterior to anterior and grows in amplitude as it travels in this direction. In Fig. 2(d) the periods of the cells are shown. The estimated periods are average values for each cell over 200 min of simulation. The period grows approximately linearly from posterior to anterior. The anteriormost period is approximately 30% longer than the posteriormost period. Because period depends on position, the phases of the cellular oscillators drift apart, resulting in the number of waves traveling the PSM increasing with time. The number of waves can be adjusted by either "cutting off" cells in the anterior (somite formation) or adding new cells in the posterior (PSM growth). This we examine in a forthcoming publication. Here we focus on the possibility of entraining these waves.

B. Entraining wave patterns in a simulated PSM by external periodic forcing

As mentioned in Sec. I, the arrest of phase waves in the presomitic mesoderm has been found to coincide with somite formation. Controlling the phase waves might thus provide a way to control the somite patterning. In this section, we investigate one way of obtaining such control, namely, by entrainment of all PSM oscillators to an external, periodic signal. The external, periodic signal we imagine to be imposed, not by something in the biological system itself, but by an outside observer, who actively wants to affect the oscillating population.

The cells are perturbed by an external periodic variation of the ν parameter (Wnt3a concentration)

$$\nu \to \nu\left[1 + K_{\text{force}} \sin\left(\frac{2\pi}{T_{\text{force}}} t\right)\right]. \tag{7}$$

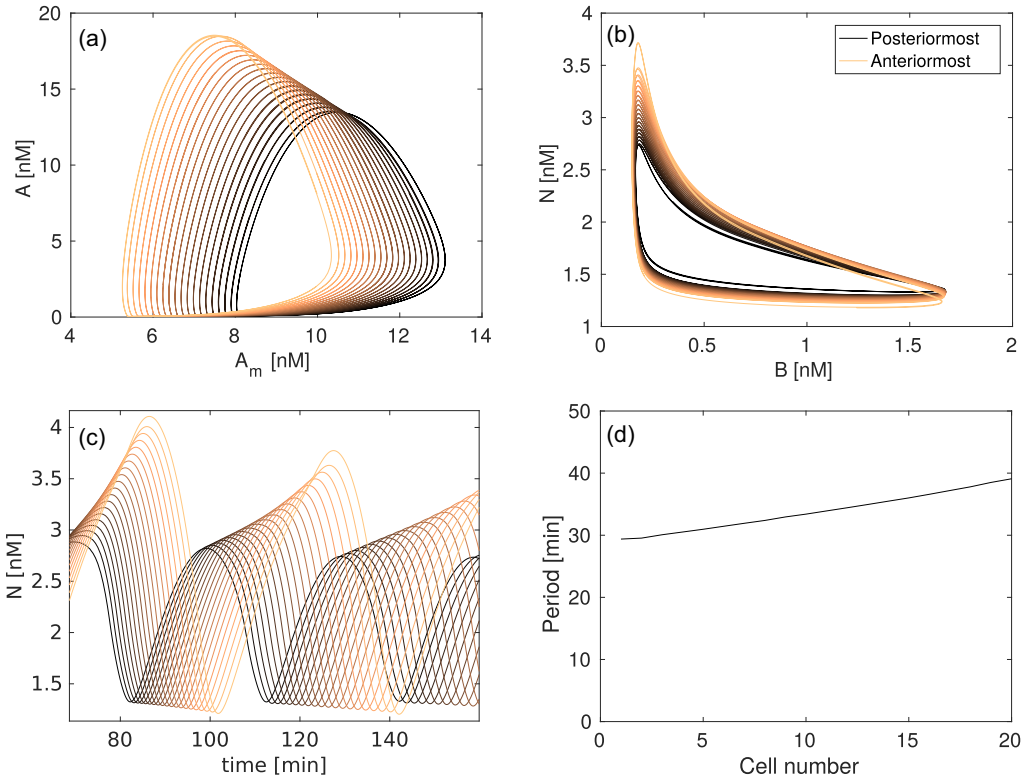

FIG. 2. *Oscillations and traveling phase waves in a PSM with a Wnt3a gradient in the absence of external periodic forcing.* Simulations of 20 cells on a line with a linear gradient in ν as described in Fig. 1 and all concentrations equal to 2 nM as initial conditions. (a, b) Plot of limit cycles for all cells. Cells located closer to the posterior end are plotted with a darker color, and those closer to the anterior end with a lighter color. The amplitude in oscillations in variables N and A increase the closer a cell is to the anterior PSM. Experimentally, the amplitude of Notch oscillations is reported to increase from posterior to anterior [42]. (c) Visualization of phase wave traveling from posterior to anterior. The amplitude in N increases from posterior to anterior. (d) Periods of PSM cells. Anterior cells have approximately 30% longer periods than posterior cells. The difference in period means that the wave pattern is not stable: the phase of the oscillators *drifts apart*.

Depending on the period (T_{force}) and the amplitude (K_{force}), the oscillations of a cell may synchronize to those of the external signal. As described above, the interval of external periods T_{force} that can entrain an oscillator to a period identical to that of an external signal is named the 1:1 Arnold tongue. We obtain 1:1 Arnold tongues in Fig. 3 for cells at three different positions, characterized by different values for the ν parameter. The leftmost Arnold tongue is for cells from the posterior PSM ($\nu = 2.500$ min^{-1}), the middle Arnold tongue is for cells from the middle of the PSM ($\nu = 2.3125$ min^{-1}), and the rightmost Arnold tongue is for cells from the anterior PSM ($\nu = 2.125$ min^{-1}). We obtained the Arnold tongues by simulating five cells on a line under the influence of each parameter pair (T_{force}, K_{force}) for 9000 min of simulations. If the oscillations of the cells were synchronized at the end of the simulation (if no neighboring cells had average periods, over the last 6000 min, which deviated more than 1 min), and if their period were identical to that of the external signal (defined as a period T_{cells} for which $|T_{\text{force}} - T_{\text{cells}}| < 0.02$ min and $T_{\text{cells}}/T_{\text{force}} < 1.01$), a 1:1 Arnold tongue was associated with the parameter pair.

The phase difference with which the cell oscillator will be entrained to the external signal depends on the position of parameters (T_{force}, K_{force}) within the Arnold tongue [23]. For an entrained cell oscillation, we measure the minimal distance between peaks of N (from any cell of the PSM) and peaks of ν, $(t_{\text{peak}\nu} - t_{\text{peak}N})/T_{\text{force}}$, and plot the results as a colormap in Fig. 3(a), overlaid on top of the previously obtained Arnold tongues. Positive values correspond to the external force peaking first.

In Fig. 3 the three Arnold tongues overlap at (T_{force}, K_{force}) = (34 min, 0.035). Hence, an external Wnt3a oscillation with these parameter values may entrain all cells in the PSM. Furthermore, with this choice of parameters, the Notch level N in posterior cells peaks before the external signal, and peaks after the external signal in anterior cells. Hence, a phase wave will travel the PSM from posterior to anterior. In Figs. 3(b) and 3(c) the limit cycles of the entrained PSM cells are shown. In this case, the amplitude of N, A, and B decrease in amplitude from posterior to anterior. In Fig. 3(d) the Notch oscillations are shown as a function of time. Phase waves travel from posterior to anterior with decreasing amplitude. In Fig. 3(e) the periods of the cells (averaged over 1000 min of simulation) are plotted. All cells have similar periods, and hence the phases of the oscillators do not drift apart. Through an external periodic variation of Wnt3a we have thus shown it is possible to obtain "external" control of the phase waves in the PSM.

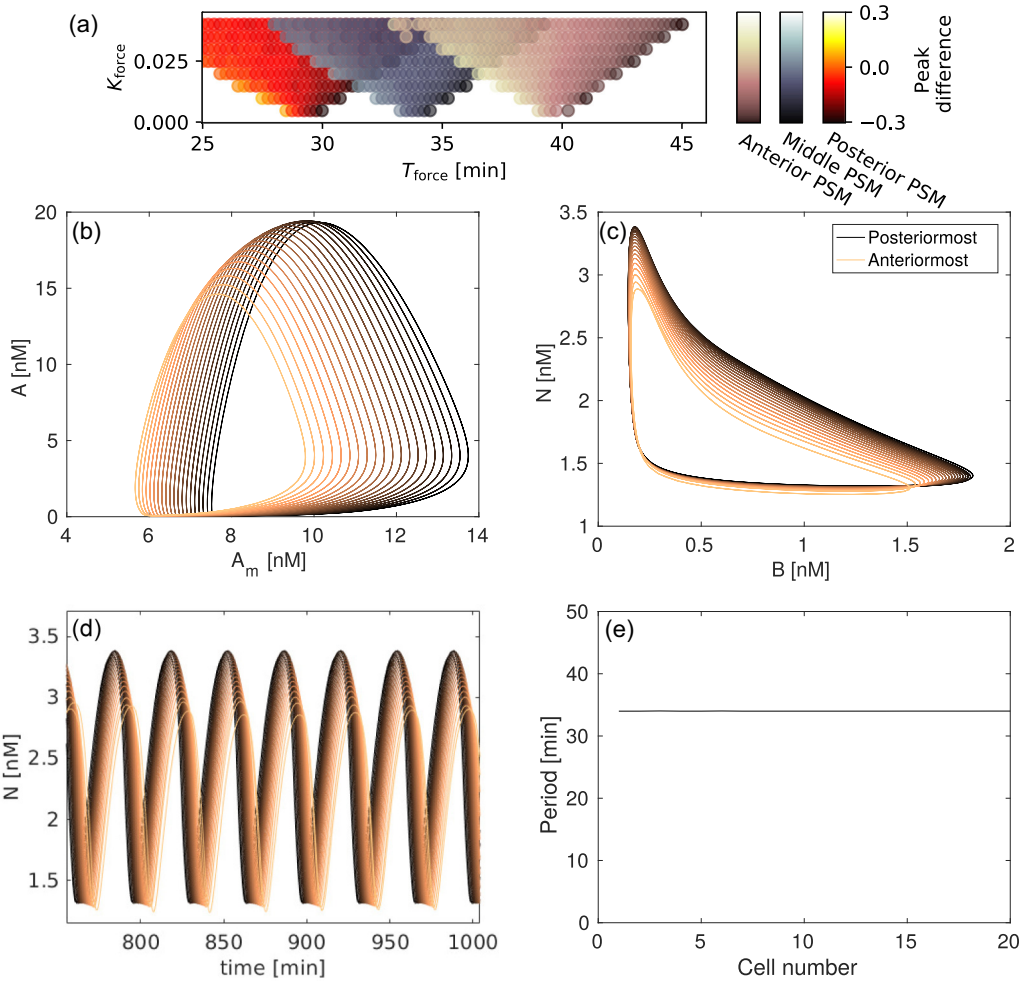

FIG. 3. *Entrainment of traveling phase waves in the presence of external periodic forcing.* (a) 1:1 Arnold tongues for cells originating from three different positions in the PSM: posterior, halfway between posterior and anterior, and anterior. The colormap indicates the value of $(t_{\text{peak}\nu} - t_{\text{peak}N})/T_{\text{force}}$. Positive values indicate that the Notch levels of cells peak after the external forcing signal. In the overlap between the three tongues, posterior cells peak before the external signal and the anterior cells peak after the external signal. Hence, a wave of maxima may travel the PSM from posterior to anterior. (b–e) A PSM, with a linear ν gradient as given by Eq. (6), under the additional influence of an external periodic forcing, as given by Eq. (7), with $(T_{\text{force}}, K_{\text{force}}) = (34\ \text{min}, 0.035)$. This parameter pair lies in the overlap between the three tongues in panel (a). (b, c) Limit cycles for each cell in the PSM under influence of the external periodic forcing. Compared to Fig. 2, the amplitude of oscillations now varies with cell position for both A and B and N. Interestingly, the amplitude is now greatest in all variables for posterior cells, not anterior cells as in Fig. 2. (d) Notch expression N of all cells as a function of time. Phase waves travel from posterior to anterior, with oscillations decreasing in amplitude with distance from the posterior end. (e) Period of cell oscillations in the phase wave of inset (d). All cells oscillate with, on average, identical period.

C. Coexisting limit cycles in PSM cells perturbed by a single external periodic signal

Properties of oscillating cells originating from similar parts of the PSM have been studied experimentally [42,49]. In these studies it was reported that the phase gradient in monolayer PSMs (an *ex vivo* culture of PSM cells that recapitulates patterning and segment scaling in the mouse PSM) decides the width of formed somites, and that mixed cells are capable of synchronizing their oscillations. In this section, we investigate the effects of a wide range of forcing parameters on cells originating from identical parts of the PSM.

We position cells on a line with the same ν parameter (i.e., we no longer have a gradient), corresponding to positions in the central part of the PSM, and vary ν periodically according to Eq. (7). To quantify whether the cell population is entrained to this external signal or not, we measure the difference between the period of the stable oscillations of the Notch concentration of the cell populations and the period of the external signal. We do this for different values of the parameters $(T_{\text{force}}, K_{\text{force}})$. The results are plotted in Fig. 4(a); colored areas in the parameter space indicate the entrainment of the oscillations of the cell population in Arnold tongues corresponding to the fraction P/Q equal to 4, 3, 2, 3/2, 1, 2/3, and 1/2. In Fig. 4(b) the oscillations of all cells are plotted along with the external forcing. All cells are entrained to the external signal.

In Fig. 4(c) the external period is approximately twice the period of the cells, which shows that the cell population has

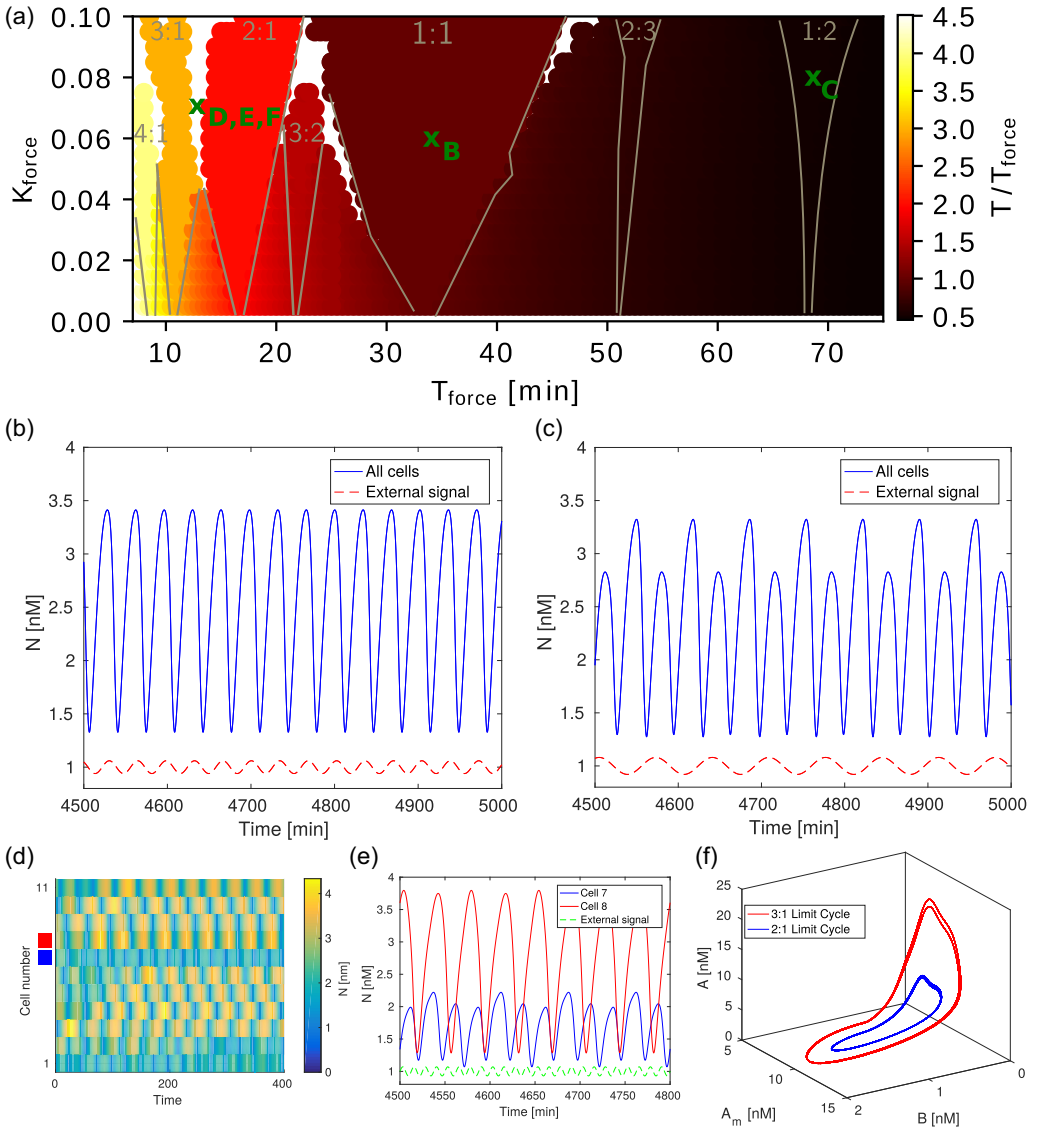

FIG. 4. *Coexistence of limit cycles induced by an external periodic forcing in the absence of a period gradient.* (a) Colormap showing the ratio of the period of a population of synchronized cells (originating from the central part of the PSM) to T_{force}, the period by which the ν level of the cells is varied. Distinct Arnold tongue structures of entrainment are clearly visible. White areas correspond to sets of parameters in which cells in the population were not synchronized after a very long time (9000 min). These areas are visible at the overlap of tongues where complex phenomena such as chaos can exist, and at the edge of the tongues where the convergence to entrainment is very slow. (b) Under the influence of an external periodic variation of the ν parameter (Wnt3a level) according to Eq. (7) with $(T_{\text{force}}, K_{\text{force}}) = (35\ \text{min}, 0.06)$ (parameter pair lies in the 1:1 tongue), 11 cells on a line synchronized their oscillations. In the simulation, all cells had $\nu = 2.3125\ \text{min}^{-1}$. The external forcing with which we multiply ν is plotted by a dashed red line. (c) Oscillations of all 11 synchronized cells with forcing parameters $(T_{\text{force}}, K_{\text{force}}) = (68\ \text{min}, 0.08)$. The forcing is shown in dashed red. Interestingly, the cells have undergone a period doubling: the maxima of the peaks alternate with double period. (d–f) Cell population under identical periodic forcing with parameters that lie between the 3:1 and 2:1 tongues, $(T_{\text{force}}, K_{\text{force}}) = (12.5\ \text{min}, 0.07)$. (d) Kymograph showing three cells entrained to one frequency or amplitude corresponding to the 2:1 tongue (blue square), and eight cells with another corresponding to the 3:1 tongue (red square). (e) Plot of Notch time series for two cells marked with squares in panel (d). Cells are entrained to different frequencies. (f) Three-dimensional projection of limit cycles that the cells can be entrained to.

undergone what is termed in the nonlinear dynamics literature as a "period doubling" [58]. Interestingly, this seems to be a general feature of the oscillations in the 1:2 tongue in our model.

Next, we investigate the behavior for parameters in the white spaces of the overlapping Arnold tongue regions in Fig. 4(a). Coexisting limit cycles in such overlapping Arnold tongues are known to exist in spin-torque oscillators affected by an injected alternating current [59] and were recently found in a system of NF-κB cells [45]. In Figs. 4(d)–4(f) we plot results obtained by performing simulations identical to the ones we performed above but with the parameters $(T_{\text{force}}, K_{\text{force}}) = (12.5\ \text{min}, 0.07)$, lying between the 2:1 and 3:1 Arnold tongues. We find that two limit cycles coexist and predict that

an experiment examining the response of a PSM cell population, taken from a single PSM location, to periodic external driving may find part of the population oscillating with one frequency while other parts oscillate with the other frequency.

From a dynamical systems perspective, the coexistence of limit cycles in certain areas in parameter space means that some bifurcation takes place on the boundary of such areas. In the sine circle map, it has previously been determined that such bifurcations are heteroclinic [60]. In the present system, however, we find that when crossing from the region in which only the 2:1-limit cycle exists, into the region in which the 2:1-limit cycle coexists with the 3:1-limit cycle, the latter limit cycle appears "out of the blue," with a finite period and amplitude. Together with the fact that we did not find any fixed points appearing or disappearing or changing in stability, this suggests that the bifurcation is a saddle-node bifurcation of cycles [58]. This is similar to what was observed in Ref. [59]. We observed coexisting limit cycles in the overlapping region between the 4:1 and 3:1 Arnold tongues as well.

IV. DISCUSSION

Locally interacting oscillating cells is a topic of fundamental interest and has been widely studied from biological, physical, and mathematical viewpoints both with and without time delays in the coupling [57,61,62]. In this paper, we use a simple limit cycle oscillator model to investigate the consequences of an external periodic variation of a morphogen gradient on a population of coupled oscillating presomitic mesoderm cells. While traveling phase waves on a line of coupled nonlinear oscillators have been well studied, to our knowledge our result that these waves can be entrained by an external periodic forcing has not been reported before. We also showed that in the context of the presomitic mesoderm such external forcing can lead to the coexistence of different limit cycles in coupled cell populations. This is to be expected due to the existence of overlapping Arnold tongues in our coupled oscillator model but is a feature that has not been observed experimentally during somitogenesis. Together, our results suggest powerful ways of controlling the spatial and temporal patterning process during somitogenesis by the relatively simple means of controlling the morphogen gradients that determine the frequency of the cellular oscillators. Such means to control the oscillations would be useful both for understanding the nonlinearities of the somitogenesis "clock" as well as the properties of the inter-cellular coupling between PSM cells.

The model we use is based on a core, negative feedback loop in the canonical Wnt pathway, and a Notch coupling between neighboring cells. The cross talk between these pathways occurs in our model via GSK3β. This remains an assumption, albeit a plausible one because experimentally GSK3β has been found to bind and phosphorylate Notch in other systems [50,51].

The Wnt oscillator is known to interact with the Notch pathway, which is known to be instrumental in coupling of cells, and this provided us a concrete way to model both the intracellular clock as well as the intercellular coupling. However, while the Wnt pathway does show oscillations, it has not been proven to be the driving clock of the PSM cells. Several other negative feedback loops exist in various somitogenesis-related pathways. It is quite possible that one of these is the main clock driving somitogenesis, as well as the oscillations in other pathways. Despite this we believe our results still provide strong "proof of principle" that external periodic variation can be used to entrain phase waves and thereby provide control of somite patterning, because synchronization, entrainment, and coexistence of multiple oscillatory modes are deep and fundamental properties of coupled oscillators that do not depend much on specific details of the oscillators [24]. Thus, we expect that even if another clock is the one driving somitogenesis, we would obtain qualitiatively similar results.

We believe our results are important for understanding the control of oscillating cell populations. We provided numerical evidence that coupled limit cycle oscillators under the influence of an external periodic force might have multiple coexisting stable limit cycles. This too depends on fundamental properties of limit cycle oscillators, and hence we expect such coexisting oscillating states to be achievable in a broad range of locally coupled, oscillating systems.

Generally, when frequencies of oscillators are proportional to spatial position along some axis, as is the case in the PSM [49], the 1:1 Arnold tongues of the cells will occupy different areas in the parameter space (T_{force}, K_{force}) of an external, periodic change in any parameter which the periods of the cells depend on. This makes control of the phase waves via entrainment possible. In the PSM, it would be very interesting to find a parameter that could be used to control the phase waves *in vivo*, because this would allow a direct and dynamic control of the spatial patterns formed during somitogenesis.

ACKNOWLEDGMENTS

We are very grateful to Alexander Aulehla and his laboratory members for valuable discussions, sharing his knowledge and results on populations of coupled PSM cells during the symposium "Biological Oscillators: Design, Mechanism, Function" at EMBL. We are also grateful to Ala Trusina for valuable discussions about Notch interactions. S.K. thanks the Simons Foundation for funding via the Simons Centre for the Study of Living Machines. M.H.J. and J.S.J. acknowledge support from the Danish Council for Independent Research (Grant No.: 4002-00395B) and StemPhys DNRF Center of Excellence (DNRF116). J.S.J. also acknowledges support from the Lørup Foundation.

[1] D. A. Hamstra, Cancer Res. **66**, 7482 (2006).
[2] M. S. Greenblatt, W. P. Bennett, M. Hollstein, and C. C. Harris, Cancer Res. **54**, 4855 (1994).
[3] D. E. Nelson, Science **306**, 704 (2004).
[4] A. Hoffmann, Science **298**, 1241 (2002).
[5] M. M. Chaturvedi, B. Sung, V. R. Yadav, R. Kannappan, and B. B. Aggarwal, Oncogene **30**, 1615 (2011).
[6] A. Aulehla and O. Pourquié, Curr. Opin. Cell Biol. **20**, 632 (2008).
[7] A. Aulehla and O. Pourquié, Brain Struct. Funct. **211**, 3 (2006).

[8] J. Cooke and E. C. Zeeman, J. Theor. Biol. **58**, 455 (1976).
[9] A. Aulehla, W. Wiegraebe, V. Baubet, M. B. Wahl, C. Deng, M. Taketo, M. Lewandoski, and O. Pourquié, Nat. Cell Biol. **10**, 186 (2008).
[10] H. Forsberg, F. Crozet, and N. A. Brown, Curr. Biol. **8**, 1027 (1998).
[11] C. Soza-Ried, E. Ozturk, D. Ish-Horowicz, and J. Lewis, Development **141**, 1780 (2014).
[12] E. M. Ozbudak and O. Pourquié, Curr. Opin. Genet. Dev. **18**, 317 (2008).
[13] Y. J. Jiang, B. L. Aerne, L. Smithers, C. Haddon, D. Ish-Horowicz, and J. Lewis, Nature (London) **408**, 475 (2000).
[14] A. Aulehla, C. Wehrle, B. Brand-Saberi, R. Kemler, A. Gossler, B. Kanzler, and B. G. Herrmann, Dev. Cell **4**, 395 (2003).
[15] A. Aulehla, Genes Dev. **18**, 2060 (2004).
[16] S. M. Reppert and D. R. Weaver, Annu. Rev. Physiol. **63**, 647 (2001).
[17] B. Pfeuty, Q. Thommen, and M. Lefranc, Biophys. J. **100**, 2557 (2011).
[18] S. Becker-Weimann, J. Wolf, H. Herzel, and A. Kramer, Biophys. J. **87**, 3023 (2004).
[19] A. Pikovsky, M. Rosenblum, and J. Kurths, *Synchronization: A Universal Concept in Nonlinear Sciences*, Cambridge Nonlinear Science Series (Cambridge University Press, Cambridge, 2003), Vol. 12.
[20] L. Glass and J. Sun, Phys. Rev. E **50**, 5077 (1994).
[21] M. H. Jensen, P. Bak, and T. Bohr, Phys. Rev. Lett. **50**, 1637 (1983).
[22] M. H. Jensen, P. Bak, and T. Bohr, Phys. Rev. A **30**, 1960 (1984).
[23] G. Bordyugov, U. Abraham, A. Granada, P. Rose, K. Imkeller, A. Kramer, and H. Herzel, J. R. Soc. Interface **12**, 20150282 (2015).
[24] V. I. Arnol'd and A. Avez, *Ergodic Problems of Classical Mechanics* (W. A. Benjamin, New York, NY, 1968).
[25] R. Kellogg and S. Tay, Cell **160**, 381 (2015).
[26] L. Glass, M. R. Guevara, J. Belair, and A. Shrier, Phys. Rev. A **29**, 1348 (1984).
[27] L. Glass, M. R. Guevara, A. Shrier, and R. Perez, Physica D **7**, 89 (1983).
[28] A. Gupta, B. Hepp, and M. Khammash, Cell Syst. **3**, 521 (2016).
[29] M. Guevara, L. Glass, and A. Shrier, Oecologia (Berlin) **19**, 75 (1975).
[30] M. H. Jensen and S. Krishna, FEBS Lett. **586**, 1664 (2012).
[31] B. M. Friedrich and F. Jülicher, Phys. Rev. Lett. **109**, 138102 (2012).
[32] K.-A. Stokkan, S. Yamazaki, H. Tei, Y. Sakaki, and M. Menaker, Science **291**, 490 (2001).
[33] A. Woller, D. Gonze, and T. Erneux, Phys. Biol. **11**, 045002 (2014).
[34] N. Mitarai, U. Alon, and M. H. Jensen, Chaos **23**, 023125 (2013).
[35] K. Kusumi, W. Sewell, and M. L. O'Brien, in *Somitogenesis*, edited by M. Maroto and N. V. Whittock, Advances in Experimental Medicine and Biology Book Series (Springer, New York, 2009), Vol. 638, pp. 140–163.
[36] K. J. Dale and O. Pourquié, BioEssays **22**, 72 (2000).
[37] J. Dubrulle, Development **131**, 5783 (2004).
[38] B. Mengel, A. Hunziker, L. Pedersen, A. Trusina, M. H. Jensen, and S. Krishna, Curr. Opin. Genet. Dev. **20**, 656 (2010).
[39] J. Cotterell, A. Robert-Moreno, and J. Sharpe, Cell Syst. **1**, 257 (2015).
[40] M. Beaupeux and P. François, Phys. Biol. **13**, 036009 (2016).
[41] I. Palmeirim, D. Henrique, D. Ish-Horowicz, and O. Pourquié, Cell **91**, 639 (1997).
[42] V. M. Lauschke, C. D. Tsiairis, P. François, and A. Aulehla, Nature (London) **493**, 101 (2012).
[43] D. Soroldoni, D. J. Jörg, L. G. Morelli, D. L. Richmond, J. Schindelin, F. Jülicher, and A. C. Oates, Science **345**, 222 (2014).
[44] K. F. Sonnen, V. M. Lauschke, J. Uraji, H. J. Falk, Y. Petersen, M. C. Funk, M. Beaupeux, P. François, C. A. Merten, and A. Aulehla, Cell **172**, 1079 (2018).
[45] M. Heltberg, R. A. Kellogg, S. Krishna, S. Tay, and M. H. Jensen, Cell Syst. **3**, 532 (2016).
[46] A. Goldbeter and O. Pourquié, J. Theor. Biol. **252**, 574 (2008).
[47] P. B. Jensen, L. Pedersen, S. Krishna, and M. H. Jensen, Biophys. J. **98**, 943 (2010).
[48] Y.-J. Jiang, L. Smithers, and J. Lewis, Curr. Biol. **8**, R868 (1998).
[49] C. Tsiairis and A. Aulehla, Cell **164**, 656 (2016).
[50] L. Espinosa, J. Ingles-Esteve, C. Aguilera, and A. Bigas, J. Biol. Chem. **278**, 32227 (2003).
[51] D. R. Foltz, M. C. Santiago, B. E. Berechid, and J. S. Nye, Curr. Biol. **12**, 1006 (2002).
[52] X. He, Dev. Cell **4**, 791 (2003).
[53] C. Y. Logan and R. Nusse, Annu. Rev. Cell Dev. Biol. **20**, 781 (2004).
[54] I. V. Chia and F. Costantini, Mol. Cell. Biol. **25**, 4371 (2005).
[55] D. S. Glass, X. Jin, and I. H. Riedel-Kruse, Phys. Rev. Lett. **116**, 128102 (2016).
[56] E. Lee, A. Salic, R. Krüger, R. Heinrich, and M. W. Kirschner, PLoS Biol. **1**, e10 (2003).
[57] S. Ares, L. G. Morelli, D. J. Jörg, A. C. Oates, and F. Jülicher, Phys. Rev. Lett. **108**, 204101 (2012).
[58] S. H. Strogatz, *Nonlinear Dynamics and Chaos: With Applications to Physics, Biology, Chemistry, and Engineering* (Westview Press, Boulder, 2014).
[59] D. Li, Y. Zhou, C. Zhou, and B. Hu, Phys. Rev. B **83**, 174424 (2011).
[60] T. Bohr and G. Gunaratne, Phys. Lett. A **113**, 55 (1985).
[61] H. Daido, Phys. Rev. Lett. **78**, 1683 (1997).
[62] H. G. Schuster and P. Wagner, Prog. Theor. Phys. **81**, 939 (1989).